Journal of Atomic, Molecular, Condensate & Nano Physics
Vol. 5, No. 1, pp. 19–39, 2018
ISSN 2349-2716 (online); 2349-6088 (print)
Published by RGN Publications

http://www.rgnpublications.com

Spectroscopic Study of EUV and SXR Transitions of Ba XLVI

Research Article

Rakesh Kumar Pandey

Department of Physics, Kirori Mal College, University of Delhi, Delhi 110007, India
r.kr.pandey@gmail.com

Abstract. An extensive set of energy levels, inverse radiative rates, wave-function composition in LSJ and JJ coupling schemes for the lowest 162 fine structure levels along with transition wavelengths, oscillator strengths, line strengths and transition probabilities for electric dipole (E1), magnetic dipole (M1), electric quadrupole (E2) and magnetic quadrupole (M2) EUV and SXR transitions from the ground state have been presented for Ba XLVI. For these calculations, the fully relativistic Multiconfiguration Dirac-Fock (MCDF) approach is employed. The QED corrections due to vacuum polarization and self-energy effects and Breit correction due to the exchange of virtual photons between two electrons are fully considered. To assess the authenticity and credibility of presented results, analogous calculations have also been performed by using a fully relativistic configuration interaction program (Flexible Atomic Code) based on self-consistent Dirac-Fock-Slater iteration method. Extreme Ultraviolet (EUV) and Soft X-ray (SXR) transitions are also identified. Comparison is also made with the available experimental and theoretical data. These accurate data are expected to be useful in fusion research and astrophysical investigations and applications.

Keywords. Energy levels; Transitions wavelength; Extreme Ultraviolet; Soft X-ray; Inverse radiative rates

PACS. 32.70.Cs; 32.30.Jc; 32.30.Rj

Received: February 27, 2018 **Accepted:** March 3, 2018

1. Introduction

During the past few decades, a continuous development in the field of atomic physics that had direct impact on other fields of research such as astrophysics, plasma physics, controlled

thermonuclear fusion, laser physics, and condensed matter physics has been witnessed. Atomic data, such as wavelengths and line identifications, are necessary for many applications, especially in plasma diagnostics and for interpreting the spectra of distant astrophysical objects.

Nowadays, investigation on the various properties of highly charged ions has received much attention due to their concernment in many research fields such as astrophysics, inertial confinement fusion (ICF), magnetic confinement fusion, laser-matter interaction, and x-ray lasers. The maximum number of lines emitted from high Z ions lies within the region of EUV (50-1200) Å and SXR (1-50) Å. The ultraviolet (UV) through EUV and soft-x-ray emission lines from multiply charged ions are particularly useful as they provide detailed knowledge of the coronal atmosphere. Substantially every observation in astronomy which involves spectra requires some aspect of atomic data for its interpretation and hence spectroscopy has become an indispensable tool to study basic plasma properties of hot astrophysical plasmas. In particular, the studies of stellar and solar coronae have intensified as a result of quality data acquisitions by the Extreme-Ultraviolet (EUV) Explorer satellite, Chandra X-ray observatory, and the Solar Heliospheric Observatory (SOHO) that recorded magnificent coronal spectra [1, 2].

Na-like ions are of considerable interest for the study and modelling of high-temperature astrophysical and laboratory plasmas, e.g. [3–7] because the adjacent neon-like stage of ionization is being used in research to develop x-ray lasers [8]. Sodium-like ions, with ground configuration $1s^2 2s^2 2p^6 3s$, have one electron outside closed shells. Thus due to their simple structure, atomic properties of sodium like ions can be calculated ab initio to high precision. The energy levels are practically free from effects of configuration mixing and therefore they are well suited for a theoretical interpretation of line intensities and for diagnostic purposes [9].

Many investigations have been carried out for the sodium like ions in the last few decades both experimentally and theoretically. Ivanov et al. [13] have calculated atomic ion energies for Na-like ions by the Model Potential method. Theodosiou et al. [14] have made calculations of lifetimes in the Na sequence by using a realistic model potential. Seely et al. [15] have reported QED contributions to the 3s-3p transitions in highly charged Na-like ions by using Grant's program. Kim et al. [16] have calculated resonance transition energies of Li, Na and Cu-like ions by relativistic many-body perturbation method. Seely et al. [17] have used Nova laser and Grant's multiconfiguration Dirac-Fock program for calculating wavelengths and energy levels for the Na I isoelectronic sequence Y^{28+} through U^{81+}. Baik et al. [18] have presented electric dipole, electric quadrupole, and magnetic dipole transition probabilities among states with principal quantum numbers $n = 3$ and 4 using Dirac-Fock single-configuration wave functions for Na-like ions in the range $56 \leq Z \leq 92$. Johnson et al. [19] have used third-order many-body perturbation theory to obtain E1 transition amplitudes for ions of the lithium and sodium isoelectronic sequences. Sapirstein et al. [20] have performed vacuum polarization calculations for hydrogen-like and alkali-metal-like ions. Further, Jiang et al. [21] have calculated resonance electron-impact excitation and polarization of the magnetic quadrupole line of neon like Ba^{46+} ions. Moreover, Sansonetti et al. [22] have compiled energy levels with designations and uncertainties for the spectra of barium $Z = 56$ ions from Ba III to Ba LVI. Gillaspy et al. [23] have used

electron beam ion trap (EBIT) and relativistic many-body perturbation theory to measure the D1 and D2 transitions in Na-like ions. Recently, Christopher J. Fontes et al. [24] have calculated relativistic distorted-wave collision strengths for all possible $\Delta n = 0$ transitions in the Li, F and Na-like ions with Z in the range $26 \leq Z \leq 92$ by using improved "top-up" method.

Barium atomic spectra have been among the first ones investigated in nearly every Electron Beam Ion Trap (EBIT) because it is used as a dopant in the electron gun cathode; as a result, its spectral lines are present along with the spectra of injected elements [10]. Spectra of Ba in the visible region have also been reported from the Livermore EBIT [11, 12]. On many EBITs, X-ray and EUV region spectra has been a subject of investigation. Therefore, in order to simulate and diagnose plasmas, accurate atomic data for different ionized barium ions, such as energy levels and transition rates, are required.

For Ba XLVI, atomic data available in the literature is limited to a few levels or transitions. Therefore, the aim of the present paper is to report data for a comparatively larger number of levels or transitions. In the present work, an extensive and highly accurate set of the energy levels, inverse radiative rates and wave-function composition for the lowest 162 fine structure levels belonging to the configurations $(1s^2 2s^2 2p^6)$ nl $(3 \leq n \leq 7;\ 0 \leq l \leq 4)$ and $(1s^2 2s^2 2p^5)\ 3l3l'$ $(l = 0, 1, 2;\ l' = 0, 1, 2)$ has been reported for Ba XLVI. Furthermore, transitions wavelengths, oscillator strengths, line strengths and transition probabilities for E1, E2, M1 and M2 EUV and SXR transitions from the ground state of Ba XLVI are also presented. QED corrections due to vacuum polarization and self-energy effects and Breit correction due to the exchange of virtual photons between two electrons are fully considered. The present calculations may be beneficial for examining new data from fusion plasma and astrophysical sources.

A brief outline of the paper is as follows. The plausibility of the present theoretical method is provided in Section 2 and results are discussed in Sections 3 and 4. Finally, concluding remarks on the present work are given in Section 5.

2. Theoretical Methods

2.1 Multi Configuration Dirac-Fock Method

For performing these large-scale calculations, fully relativistic MCDF method revised by Norrington [25] formerly developed by Grant et al. [26] is applied. QED corrections due to self-energy and vacuum polarization effects and Breit corrections due to the exchange of virtual photons as a first order perturbation theory have also been considered. Since the elaborate depiction of this method has been presented elsewhere [25, 27–30], so only a brief outline is discussed here. The Dirac-Coulomb Hamiltonian in MCDF approach for an N-electron atom or ion can be written as follows

$$\widehat{H}^{DC} = \sum_{i=1}^{N} \widehat{H}_i + \sum_{i=1}^{N-1} \sum_{j=i+1}^{N} \frac{1}{|\widehat{r}_i - \widehat{r}_j|}, \tag{2.1}$$

where $\widehat{H}$, the one-electron Hamiltonian is given by

$$\widehat{H}_i = c\vec{\alpha} i \cdot \vec{p}_i + \beta mc^2 + V_{nuc}\,. \tag{2.2}$$

In equation (2.2) first two terms signify kinetic energy of an electron and the last term represents the Coulomb potential of the nucleus. α and β are 4×4 Dirac matrices and c is the speed of light. The N electron wave function constructed from central-field Dirac orbitals is given by

$$\phi_{nkm}=\frac{1}{r}\begin{pmatrix} P_nk(r) & \chi_{km}(\theta,\phi,\sigma)\\ -iQ_nk(r) & \chi_{-km}(\theta,\phi,\sigma)\end{pmatrix}, \tag{2.3}$$

where k is the Dirac angular quantum number, $k=\pm(j+1/2)$ for $l=j\pm1/2$, so $j=k-1/2$, m is the projection of the angular momentum j, and P_{nk} and Q_{nk} are large and small components of one electron radial functions. The spin angular momentum χ_{km} (θ,ϕ) is a 2 component function defined by

$$\chi_{km}(\theta,\phi)=\sum_{\sigma=\pm\frac{1}{2}}\left\langle lm-\sigma\frac{1}{2}\sigma\middle|l\frac{1}{2}jm\right\rangle Y_l^{m-\sigma}(\theta,\phi)\phi^{\sigma}\,. \tag{2.4}$$

An atomic state function (ASF) for N electron system constructed by the linear combination of n electronic configuration state functions (CSFs) is represented by

$$|\psi_\alpha(PJM)\rangle=\sum_{i=1}^{n}C_i(\alpha)|\gamma_i(PJM)\rangle\,, \tag{2.5}$$

where $C_i(\alpha)$ are the expansion mixing coefficients for each CSF and satisfy the relation

$$(C_i(\alpha))^{\dagger}C_j(\alpha)=\delta_{ij}\,. \tag{2.6}$$

Such that ASFs satisfy the orthonormality condition. α represents the orbital occupation numbers, coupling, etc. and $\gamma_i(PJM)$ are CSFs which specify a particular state with a given parity and angular momentum (J,M).

In equation (2.6), the basis wave-functions are enlarged by considering the important correlations and relativistic effects. CSFs of particular parity P and symmetry have been generated by taking appropriate excitations from reference configurations to higher shells.

By taking expectation value of the Dirac-Hamiltonian, we get energy of the N-electron system as

$$\begin{aligned} E_\alpha^P JM&=\langle\psi_\alpha(PJM)|H^{DC}|\psi_\alpha(PJM)\rangle\\ &=\sum_{ij}C_i^*(\alpha)C_i(\alpha)\langle\gamma_i(PJM)|H^{DC}|\gamma_j(PJM)\rangle\\ &=(C_\alpha^{DC})^{\dagger}H^{DC}C_\alpha^{DC}\,. \end{aligned} \tag{2.7}$$

The elements of Dirac Hamiltonian matrix H^{DC} are given by

$$H_{rs}^{DC}=\langle\gamma_r(PJM)|H^{DC}|\gamma_s(PJM)\rangle\,. \tag{2.8}$$

Using the condition of normalization

$$(H^{DC}-E_\alpha^{DC}I)C_\alpha^{DC}=0\,, \tag{2.9}$$

where I is the $(n\times n)$ unit matrix. Thus the predicted atomic energy level E_α^{PJM} can be taken to be eigenvalues of H^{DC}.

2.2 FAC Calculations

To illustrate the accuracy of calculated results from MCDF, parallel calculations have also been carried out using fully relativistic configuration interaction method, based on self-consistent Dirac-Fock-Slater iteration performed on a selected fictitious mean configuration in order to derive the local central potential [31, 32]. In Flexible Atomic Code (FAC), the orbitals are optimized self consistently and the average energy of a fictitious mean configuration with orbital occupation numbers is minimized. Using FAC, larger calculations up to 2718 fine structure levels belonging to $(2*8)3*1$, $4*1$, $5*1$, $6*1$, $7*1$ and $(2*7)3*2$, $4*2$, $3*1\ 4*1$, $3*1\ 5*1$ configurations have been performed. These results are listed in Table 2.

3. Results and Discussion

3.1 Energy Levels

The basic procedure for the determination of accurate and complete atomic data, namely, energy levels, lifetimes, oscillator strength, etc. for highly stripped ions is configuration interaction. In the present work, the lowest 162 fine-structure levels for Ba XLVI are reported by performing Multi Configuration Dirac-Fock calculations up to 2718 levels. In these calculations, all the major correlations namely internal, semi-internal and external are incorporated. The configurations included are $2p^6nl$ with $3 \le n \le 7$ and $0 \le l \le 4$, $2p^53l\ nl'$ $(3 \le n \le 5)$, $2p^54l\ nl'$ $(4 \le n \le 5)$, $2s2p^6\ 3l\ nl'$ $(3 \le n \le 4)$ and $2s2p^6\ 4l\ 4l'$. In Table 1, the lowest 162 fine structure levels with the wave-functions composition in JJ and LSJ coupling under the column "composition" have been listed. In Table 1, indices in the first column "Level No." represent the level number and configurations in LSJ coupling are presented in the second column. For simplicity, $1s^2$ core has been excluded in the notation of configurations. In the column "JJ coupling" of Table 1, the first number represents the leading percentage of the level and notations p^-, p, d, d^-, f, f^-, g and g^- denotes $p_{1/2}$, $p_{3/2}$, $d_{5/2}$, $d_{3/2}$, $f_{7/2}$, $f_{5/2}$, $g_{9/2}$ and $g_{7/2}$, respectively. Similarly, in the last column "LSJ coupling" the first number indicates the leading percentage of level corresponding to the level number in the first column "Level No." and next leading percentages are presented in the format of X (Y), where X represents the percentage of level corresponding to level number Y. In our MCDF calculations, for lowest 40 levels there is no mixing in LSJ. In present MCDF calculations, mixing among some levels in LSJ coupling is very strong. For example, for level number 46, $2p^53s3p^2P_{3/2}$ is strongly mixed with $2p^53s3p\ ^4S_{3/2}$ and $2p^53s3p\ ^2P_{3/2}$ with their composition as 30%, 29% and 25%, respectively. Similarly, there are several other cases, as can be seen from Table 1. Therefore, due to this mixing effect, definite recognition of levels is a very difficult task.

In Table 2, energies in Ryd. for the lowest 162 fine-structure energy levels for Ba XLVI have been reported.Moreover, contribution of DC, Breit as well as QED corrections to total energy are also listed. It can be seen that QED corrections are comparable to Breit corrections for configurations due to single electron excitation. On the other hand, the effect of QED corrections is negligible in comparison to Breit corrections for other higher configurations. Hence, it can be concluded that QED corrections are significant for highly ionized high Z ions. Results from FAC are also presented in Table 2. In Table 3, comparisons have also been made between

the energies calculated from MCDF and FAC for lowest 21 levels with the data compiled by NIST [33], Baik et al. [18] and Ivanov et al. [13]. The differences between experimental energy levels and the present MCDF/FAC ones are shown in Figure 1. One can see that the results from both calculations (MCDF and FAC) are not only in good agreement with all available results but are also very close to NIST which ensures the credibility of presented results.

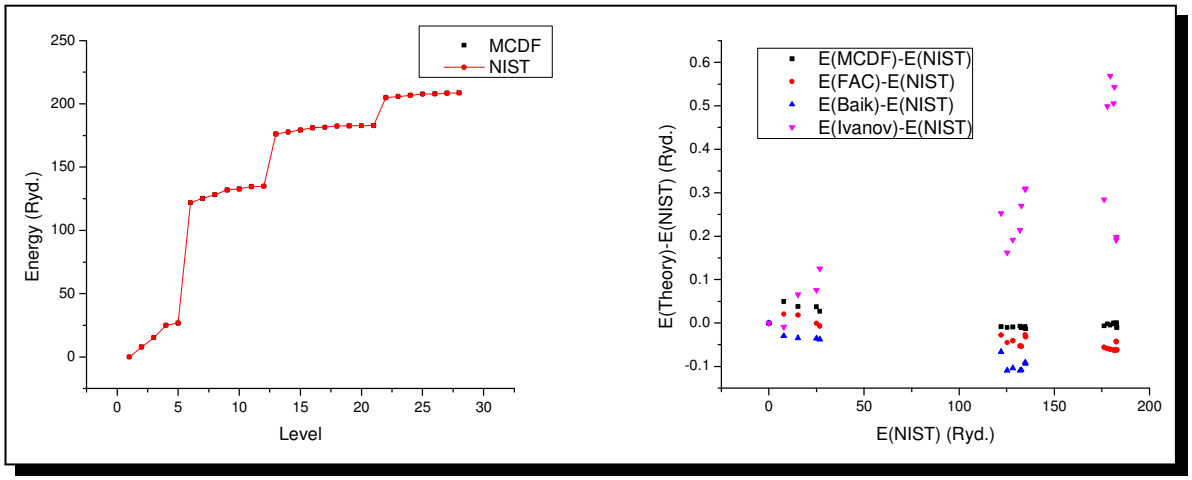

Figure 1. Comparison of MCDF and NIST energies for Ba XLVI using Table 3

One can calculate the uncertainty in the energies of fine structure levels with observed level energies by the following relation

$$\Delta E = \frac{(E_{NIST.} - E_{MCDF.})}{E_{NIST}} \times 100\% \tag{3.1}$$

The maximum deviation between MCDF energies and energies compiled by NIST is 0.0497 Ryd. for level $2p^6 3p\ {}^2P^o_{1/2}$ and this deviation and graphical comparison in Figure 1 shows that a good agreement is achieved with the NIST.

3.2 Radiative Data of EUV and SXR Transitions

Absorption oscillator strength (f_{ij}) for a transition $i \rightarrow j$ is related to the radiative rate A_{ji} (in $s-1$) by the following expression

$$f_{ij} = \frac{mc\lambda_{ji}^2}{8\pi^2 e^2}\frac{\omega_j}{\omega_i}A_{ji}\,, \tag{3.2}$$

where m, c and e are the mass of electron, velocity of light and electron charge respectively. Also, λ_{ji} is the transition wavelength in Å and ω_j, ω_i denotes statistical weights of the upper and lower levels, respectively. In Table 4-7, the transition wavelength, radiative rate, oscillator strength and line strength for all E1, E2, M1 and M2 transitions from ground state among the lowest 162 levels of Ba XLVI have been presented. The results are presented only in the length form as the results in Babushkin gauge is assumed to be more accurate and precise as compared to that in Coulomb gauge [34–36]. The indices for the notation of lower level i and upper level j are mentioned in the first column of Table 1.

A desirable but not a necessary condition to judge the accuracy of calculated radiative data is the agreement between length and velocity form of radiative data. Therefore velocity gauge/length gauge ratios of results of absorption oscillator strength for E1 and E2 transitions are listed in the last column of Table 4 and 5. From Table 4 and 5, one can see that in most of the cases, the ratio is exactly unity for some transitions such as 1-7, 1-8 etc. for E1 transitions and transitions number 9 and 10 for E2 transitions the ratios are far from unity due to the effect of internal cancellation in radiation transition integrals [37]. From Table 4-7, we have identified 2 EUV and 79 SXR spectral lines in dipole transitions, 1 EUV and 84 SXR spectral lines in quadrupole transitions. In Figure 2 and 3, we have plotted gA spectra of E1, E2 and M1, M2 SXR transitions respectively. From Figure 2, we predicted that gA is maximum for the E1 SXR transitions having wavelengths lying around 2.5 Å while for E2 transitions it lies around 2.6 Å and from Figure 3, we observed that the value of gA is maximum for the M1 SXR transitions having wavelengths lying around 2.5 Å while for M2 transitions it lies below 2.7 Å. The actual value of peaks can be determined from Table 4-7.

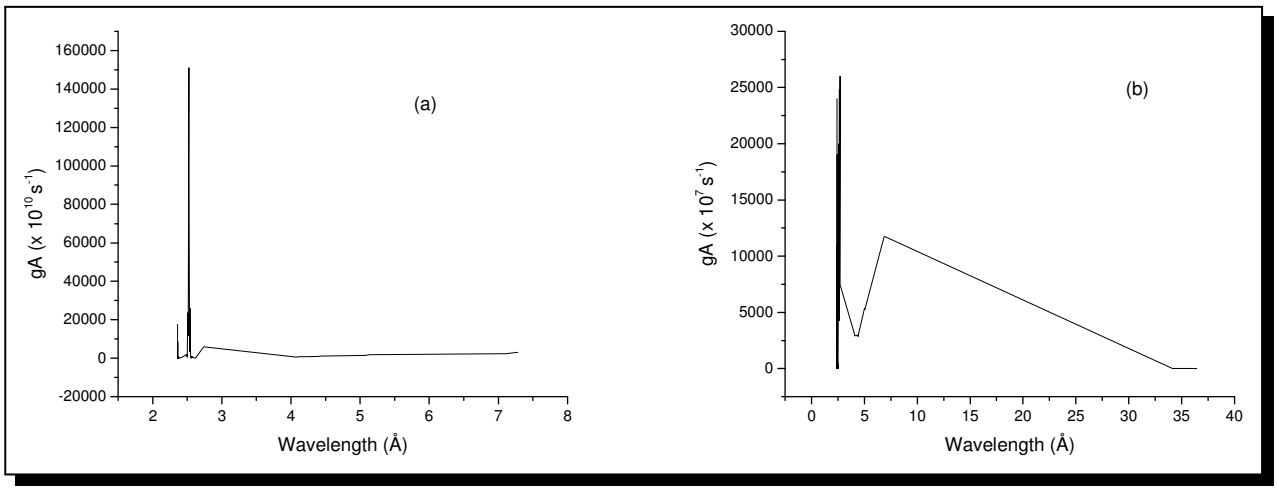

Figure 2. gA spectra of (a) E1 and (b) E2 SXR transitions from the ground state

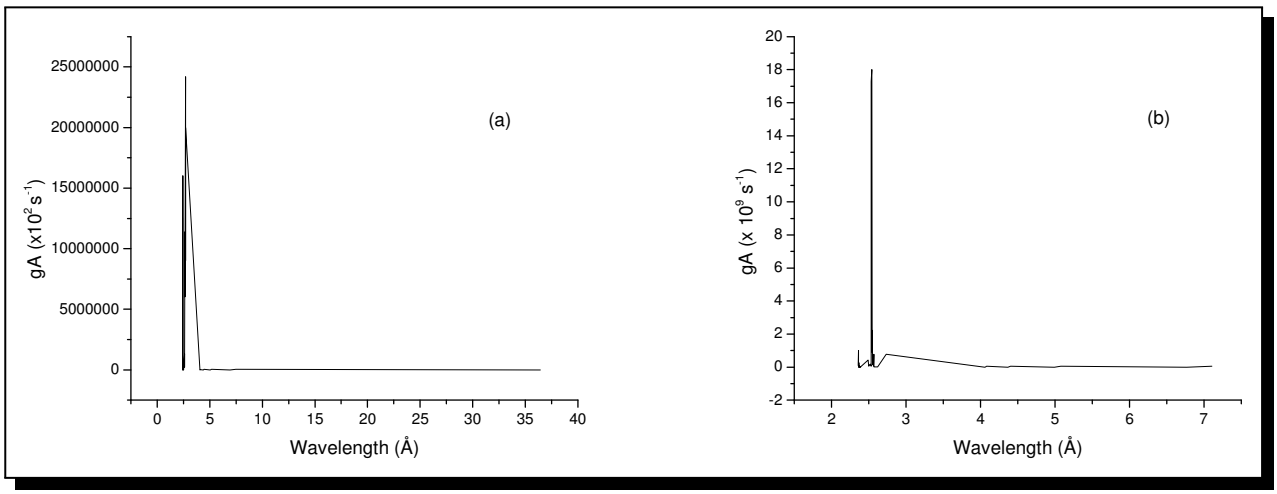

Figure 3. gA spectra of (a) M1 and (b) M2 SXR transitions from the ground state

Table 1. Level No., Wave-function compositions and inverse radiative rates of first 162 fine structure levels of Ba XLVI ($aE \pm b = a \times 10^{\pm b}$)

Level No.	Configurations	$(\Sigma A_r)^{-1}$ (in s)	Composition	
			JJ coupling	LSJ coupling
1	$2p^6 3s\ ^2S_{1/2}$	--------	**100** $2p^{-2}2p^4 3s$	100
2	$2p^6 3p\ ^2P^o_{1/2}$	3.9216E-11	**100** $2p^{-2}2p^4 3p^{-1}$	100
3	$2p^6 3p\ ^2P^o_{3/2}$	4.9999E-12	**100** $2p^{-2}2p^4 3p$	100
4	$2p^6 3d\ ^2D_{3/2}$	4.7548E-12	**100** $2p^{-2}2p^4 3d^{-1}$	100
5	$2p^6 3d\ ^2D_{5/2}$	1.3885E-11	**100** $2p^{-2}2p^4 3d$	100
6	$2p^6 4s\ ^2S_{1/2}$	6.0595E-14	**100** $2p^{-2}2p^4 4s$	100
7	$2p^6 4p\ ^2P^o_{1/2}$	5.1343E-14	**100** $2p^{-2}2p^4 4p^{-1}$	100
8	$2p^6 4p\ ^2P^o_{3/2}$	6.5060E-14	**100** $2p^{-2}2p^4 4p$	100
9	$2p^6 4d\ ^2D_{3/2}$	3.1852E-14	**100** $2p^{-2}2p^4 4d^{-1}$	100
10	$2p^6 4d\ ^2D_{5/2}$	3.1261E-14	**100** $2p^{-2}2p^4 4d$	100
11	$2p^6 4f\ ^2F^o_{5/2}$	1.5295E-14	**100** $2p^{-2}2p^4 4f^{-1}$	100
12	$2p^6 4f\ ^2F^o_{7/2}$	1.5506E-14	**100** $2p^{-2}2p^4 4f$	100
13	$2p^6 5s\ ^2S_{1/2}$	7.3954E-14	**100** $2p^{-2}2p^4 5s$	100
14	$2p^6 5p\ ^2P^o_{1/2}$	6.3273E-14	**100** $2p^{-2}2p^4 5p^{-1}$	100
15	$2p^6 5p\ ^2P^o_{3/2}$	7.7821E-14	**100** $2p^{-2}2p^4 5p$	100
16	$2p^6 5d\ ^2D_{3/2}$	4.2995E-14	**100** $2p^{-2}2p^4 5d^{-1}$	100
17	$2p^6 5d\ ^2D_{5/2}$	4.2656E-14	**100** $2p^{-2}2p^4 5d$	100
18	$2p^6 5f\ ^2F^o_{5/2}$	2.8916E-14	**100** $2p^{-2}2p^4 5f^{-1}$	100
19	$2p^6 5f\ ^2F^o_{7/2}$	2.9394E-14	**100** $2p^{-2}2p^4 5f$	100
20	$2p^6 5g\ ^2G_{7/2}$	5.1808E-14	**100** $2p^{-2}2p^4 5g^{-1}$	100
21	$2p^6 5g\ ^2G_{9/2}$	5.2028E-14	**100** $2p^{-2}2p^4 5g$	100
22	$2p^6 6s\ ^2S_{1/2}$	1.0237E-13	**100** $2p^{-2}2p^4 6s$	100
23	$2p^6 6p\ ^2P^o_{1/2}$	8.8704E-14	**100** $2p^{-2}2p^4 6p^{-1}$	100
24	$2p^6 6p\ ^2P^o_{3/2}$	1.0693E-13	**100** $2p^{-2}2p^4 6p$	100
25	$2p^6 6d\ ^2D_{3/2}$	6.3334E-14	**100** $2p^{-2}2p^4 6d^{-1}$	100
26	$2p^6 6d\ ^2D_{5/2}$	6.3491E-14	**100** $2p^{-2}2p^4 6d$	100
27	$2p^6 6f\ ^2F^o_{5/2}$	4.8436E-14	**100** $2p^{-2}2p^4 6f^{-1}$	100
28	$2p^6 6f\ ^2F^o_{7/2}$	4.9369E-14	**100** $2p^{-2}2p^4 6f$	100
29	$2p^6 6g\ ^2G_{7/2}$	8.7445E-14	**100** $2p^{-2}2p^4 6g^{-1}$	100
30	$2p^6 6g\ ^2G_{9/2}$	8.7998E-14	**100** $2p^{-2}2p^4 6g$	100
31	$2p^6 7s\ ^2S_{1/2}$	1.3390E-13	**100** $2p^{-2}2p^4 7s$	100
32	$2p^6 7p\ ^2P^o_{1/2}$	1.1705E-13	**100** $2p^{-2}2p^4 7p^{-1}$	100
33	$2p^6 7p\ ^2P^o_{3/2}$	1.3718E-13	**100** $2p^{-2}2p^4 7p$	100
34	$2p^6 7d\ ^2D_{3/2}$	8.7377E-14	**100** $2p^{-2}2p^4 7d^{-1}$	100
35	$2p^6 7d\ ^2D_{5/2}$	8.8678E-14	**100** $2p^{-2}2p^4 7d$	100
36	$2p^6 7f\ ^2F^o_{5/2}$	7.4080E-14	**100** $2p^{-2}2p^4 7f^{-1}$	100
37	$2p^6 7f\ ^2F^o_{7/2}$	7.5387E-14	**100** $2p^{-2}2p^4 7f$	100
38	$2p^6 7g\ ^2G_{7/2}$	1.3724E-13	**100** $2p^{-2}2p^4 7g^{-1}$	100
39	$2p^6 7g\ ^2G_{9/2}$	1.3808E-13	**100** $2p^{-2}2p^4 7g$	100
40	$2p^5 3s^2\ ^2P^o_{3/2}$	3.3377E-14	**99** $2p^{-2}2p^3 3s^2$	99
41	$2p^5 3s\ (^3P)\ 3p\ ^4P_{3/2}$	2.7198E-13	**90** $2p^{-2}2p^3 3s(2)3p^{-1}$	41+26(120)+19(95)
42	$2p^5 3s\ (^3P)\ 3p\ ^4D_{5/2}$	1.9796E-12	**98** $2p^{-2}2p^3 3s(2)3p^{-1}$	47+33(50)+19(47)
43	$2p^5 3s\ (^1P)\ 3p\ ^2D_{3/2}$	2.8355E-14	**89** $2p^{-2}2p^3 3s(1)3p^{-1}$	51
44	$2p^5 3s\ (^1P)\ 3p\ ^2P_{1/2}$	2.7143E-14	**99** $2p^{-2}2p^3 3s(1)3p^{-1}$	43+22(48)+20(98)
45	$2p^5 3s\ (^3P)\ 3p\ ^4D_{7/2}$	3.1732E-09	**100** $2p^{-2}2p^3 3s(2)3p$	100
46	$2p^5 3s\ (^1P)\ 3p\ ^2P_{3/2}$	4.7038E-14	**60** $2p^{-2}2p^3 3s(1)3p$	30+29(120)+25(51)
47	$2p^5 3s\ (^3P)\ 3p\ ^4P_{5/2}$	5.9787E-14	**57** $2p^{-2}2p^3 3s(2)3p$	59+28(122)
48	$2p^5 3s\ (^1P)\ 3p\ ^2S_{1/2}$	3.3381E-14	**83** $2p^{-2}2p^3 3s(1)3p$	39+32(128)+17(44)
49	$2p^5 3p^2\ ^4P^o_{3/2}$	1.3512E-12	**98** $2p^{-2}2p^3 3p^{-2}$	22+27(83)+20(144)
50	$2p^5 3s\ (^3P)\ 3p\ ^2D_{5/2}$	4.4943E-14	**56** $2p^{-2}2p^3 3s(1)3p$	45+37(122)
51	$2p^5 3s\ (^3P)\ 3p\ ^2P_{3/2}$	4.8142E-14	**57** $2p^{-2}2p^3 3s(2)3p$	40+25(46)+24(130)
52	$2p^5 3s\ (^3P)\ 3p\ ^2S_{1/2}$	7.0858E-14	**81** $2p^{-2}2p^3 3s(2)3p$	52+24(98)
53	$2p^5 3p^2\ ^2S^o_{1/2}$	1.8737E-13	**60** $2p^{-2}2p^3 3p^{-1}3p$	21+29(78)+24(141)
54	$2p^5 3p^2\ ^4P^o_{5/2}$	2.1374E-12	**91** $2p^{-2}2p^3 3p^{-1}3p$	45

55	$2p^5\,3p^2\ {}^2P^o_{3/2}$	1.4217E-13	**49**	$2p^{-2}2p^3 3p^{-1}3p$	27+25(87)
56	$2p^5\,3p^2\ {}^2F^o_{7/2}$	7.9788E-13	**84**	$2p^{-2}2p^3 3p^{-1}3p$	57+27(77)
57	$2p^5\,3p^2\ {}^2D^o_{3/2}$	5.4372E-13	**50**	$2p^{-2}2p^3 3p^{-1}3p$	34+21(49)
58	$2p^5\,3p^2\ {}^2D^o_{5/2}$	4.1356E-13	**84**	$2p^{-2}2p^3 3p^{-1}3p$	23+33(79)
59	$2p^5 3s\ (^3P)\ 3d\ {}^4P^o_{1/2}$	4.9344E-13	**89**	$2p^{-2}2p^3 3s(2)3d^{-1}$	88
60	$2p^5 3s\ (^3P)\ 3d\ {}^4P^o_{3/2}$	9.5206E-13	**86**	$2p^{-2}2p^3 3s(2)3d^{-1}$	64
61	$2p^5 3s\ (^1P)\ 3d\ {}^2P^o_{1/2}$	3.3956E-14	**57**	$2p^{-2}2p^3 3s(1)3d^{-1}$	38
62	$2p^5 3s\ (^3P)\ 3d\ {}^4F^o_{5/2}$	6.4426E-14	**62**	$2p^{-2}2p^3 3s(2)3p^{-1}$	38+23(64)+22(161)
63	$2p^5 3s\ (^3P)\ 3d\ {}^4F^o_{7/2}$	3.1767E-13	**81**	$2p^{-2}2p^3 3s(2)3d^{-1}$	57+21(70)
64	$2p^5 3s\ (^3P)\ 3d\ {}^4D^o_{5/2}$	5.1537E-14	**54**	$2p^{-2}2p^3 3s(1)3d^{-1}$	32+34(161)
65	$2p^5 3s\ (^1P)\ 3d\ {}^2D^o_{3/2}$	2.6273E-14	**86**	$2p^{-2}2p^3 3s(1)3d^{-1}$	50+19(159)
66	$2p^5 3s\ (^3P)\ 3d\ {}^4F^o_{9/2}$	1.3869E-11	**100**	$2p^{-2}2p^3 3s(2)3d$	100
67	$2p^5 3p^2\ {}^2P^o_{1/2}$	7.2967E-15	**34**	$2p^{-2}2p^3 3p^{-1}3p$	24+29(78)+18(61)
69	$2p^5 3s\ (^3P)\ 3d\ {}^4D^o_{7/2}$	6.4595E-14	**60**	$2p^{-2}2p^3 3s(2)3d$	65
70	$2p^5 3s\ (^3P)\ 3d\ {}^2F^o_{7/2}$	6.3492E-14	**46**	$2p^{-2}2p^3 3s(1)3d$	41+18(77)
71	$2p^5 3s\ (^3P)\ 3d\ {}^2D^o_{3/2}$	2.5173E-14	**57**	$2p^{-2}2p^3 3s(1)3d$	39
72	$2p^5 3s\ (^1P)\ 3d\ {}^2D^o_{5/2}$	4.3838E-14	**49**	$2p^{-2}2p^3 3s(1)3d$	32+20(68)
73	$2p^5 3s\ (^3P)\ 3d\ {}^2P^o_{1/2}$	1.9919E-15	**58**	$2p^{-2}2p^3 3s(2)3d$	45+20(75)
74	$2p^5 3s\ (^3P)\ 3d\ {}^2P^o_{3/2}$	1.2894E-15	**45**	$2p^{-2}2p^3 3s(2)3d$	40
75	$2p^5 3s^2\ {}^2P^o_{1/2}$	1.6861E-14	**73**	$2p^{-1}\,2p^4 3s^2$	73
76	$2p^5 3p\ (^3P)\ 3d\ {}^4D_{1/2}$	3.6239E-13	**86**	$2p^{-2}2p^3 3p^{-1}(1)3d^{-1}$	40
77	$2p^5 3p^2\ {}^4D^o_{7/2}$	5.3339E-13	**89**	$2p^{-2}\,2p^3 3p^2$	51+40(56)
78	$2p^5 3p^2\ {}^2P^o_{1/2}$	8.4317E-15	**71**	$2p^{-2}\,2p^3 3p^2$	32+22(53)+18(73)
79	$2p^5 3p^2\ {}^2D^o_{5/2}$	2.0983E-13	**84**	$2p^{-2}\,2p^3 3p^2$	33+24(54)+17(58)
80	$2p^5 3p\ (^3S)\ 3d\ {}^4D_{3/2}$	1.7739E-13	**67**	$2p^{-2}2p^3 3p^{-1}(1)3d^{-1}$	24+19(107)
81	$2p^5 3p\ (^3D)\ 3d\ {}^4G_{7/2}$	6.1022E-12	**100**	$2p^{-2}2p^3 3p^{-1}(2)3d^{-1}$	30
82	$2p^5 3p\ (^3P)\ 3d\ {}^4F_{5/2}$	9.5985E-12	**55**	$2p^{-2}2p^3 3p^{-1}(1)3d^{-1}$	25
83	$2p^5 3p^2\ {}^2P^o_{3/2}$	2.4501E-13	**87**	$2p^{-2}\,2p^3 3p^2$	63
84	$2p^5 3p\ (^3D)\ 3d\ {}^4P_{1/2}$	4.5166E-13	**82**	$2p^{-2}2p^3 3p^{-1}(2)3d^{-1}$	34+21(110)+17(116)
85	$2p^5 3p\ (^3D)\ 3d\ {}^4F_{5/2}$	2.2471E-12	**55**	$2p^{-2}2p^3 3p^{-1}(2)3d^{-1}$	17
86	$2p^5 3p\ (^3D)\ 3d\ {}^4D_{3/2}$	5.1954E-13	**63**	$2p^{-2}2p^3 3p^{-1}(2)3d^{-1}$	20
87	$2p^5 3p^2\ {}^2D^o_{3/2}$	8.0414E-14	**85**	$2p^{-2}\,2p^3 3p^2$	19+28(156)
88	$2p^5 3p\ (^3P)\ 3d\ {}^4F_{7/2}$	9.1243E-12	**88**	$2p^{-2}2p^3 3p^{-1}(1)3d$	19+30(111)+21(114)
89	$2p^5 3p\ (^3D)\ 3d\ {}^4G_{9/2}$	5.4183E-12	**96**	$2p^{-2}2p^3 3p^{-1}(2)3d$	43+17(113)
90	$2p^5 3p\ (^3P)\ 3d\ {}^2P_{3/2}$	5.7512E-13	**48**	$2p^{-2}2p^3 3p^{-1}(1)3d$	18
91	$2p^5 3p\ (^3P)\ 3d\ {}^2F_{5/2}$	2.6892E-12	**53**	$2p^{-2}2p^3 3p^{-1}(1)3d$	16
92	$2p^5 3p\ (^3P)\ 3d\ {}^4P_{5/2}$	5.5610E-12	**56**	$2p^{-2}2p^3 3p^{-1}(2)3d$	18
93	$2p^5 3p\ (^1D)\ 3d\ {}^2F_{7/2}$	5.0917E-12	**87**	$2p^{-2}2p^3 3p^{-1}(2)3d$	24
94	$2p^5 3s\ (^3P)\ 3p\ {}^4D_{1/2}$	7.6634E-15	**50**	$2p^{-1}2p^4 3s(0)3p^{-1}$	60
95	$2p^5 3s\ (^3P)\ 3p\ {}^4D_{3/2}$	2.0403E-15	**31**	$2p^{-2}2p^3 3p^{-1}(2)3d$	13
96	$2p^5 3p\ (^3P)\ 3d\ {}^2P_{1/2}$	1.4813E-15	**72**	$2p^{-2}2p^3 3p^{-1}(2)3d$	16
97	a	4.0476E-15	**67**	$2p^{-1}2p^4 3s(1)3p^{-1}$	
98	$2p^5 3s\ (^3P)\ 3p\ {}^4P_{1/2}$	1.3405E-13	**64**	$2p^{-1}2p^4 3s(1)3p^{-1}$	43+26(52)
99	$2p^5 3p\ (^3D)\ 3d\ {}^4P_{3/2}$	8.9171E-14	**62**	$2p^{-2}2p^3 3p(3)3d^{-1}$	35
100	$2p^5 3p\ (^1P)\ 3d\ {}^2P_{1/2}$	2.8317E-13	**69**	$2p^{-2}2p^3 3p(1)3d^{-1}$	39
101	$2p^5 3p\ (^3D)\ 3d\ {}^4D_{5/2}$	1.4444E-12	**68**	$2p^{-2}2p^3 3p(3)3d^{-1}$	36
102	$2p^5 3p\ (^3D)\ 3d\ {}^2F_{7/2}$	2.4627E-12	**82**	$2p^{-2}2p^3 3p(3)3d^{-1}$	32
104	$2p^5 3p\ (^1P)\ 3d\ {}^2D_{3/2}$	3.9842E-14	**52**	$2p^{-2}2p^3 3p(1)3d^{-1}$	22
105	$2p^5 3p\ (^3D)\ 3d\ {}^4F_{9/2}$	2.7965E-12	**85**	$2p^{-2}2p^3 3p(3)3d^{-1}$	36+33(117)+27(89)
106	$2p^5 3p\ (^3D)\ 3d\ {}^4G_{11/2}$	6.3283E-12	**100**	$2p^{-2}2p^3 3p(3)3d$	100
107	$2p^5 3p\ (^3P)\ 3d\ {}^4D_{3/2}$	3.3105E-13	**65**	$2p^{-2}2p^3 3p(2)3d^{-1}$	20
108	$2p^5 3p\ (^3D)\ 3d\ {}^4D_{7/2}$	2.4043E-12	**56**	$2p^{-2}2p^3 3p(2)3d^{-1}$	26
109	$2p^5 3p\ (^3P)\ 3d\ {}^4D_{5/2}$	2.9438E-13	**70**	$2p^{-2}2p^3 3p(2)3d^{-1}$	25
110	$2p^5 3p\ (^3P)\ 3d\ {}^4P_{1/2}$	1.3099E-13	**72**	$2p^{-2}2p^3 3p(2)3d^{-1}$	33
111	$2p^5 3p\ (^3S)\ 3d\ {}^4D_{7/2}$	3.6943E-12	**68**	$2p^{-2}2p^3 3p(1)3d$	26+37(118)

112	$2p^5 3p\ (^1P)\ 3d\ ^2D_{5/2}$	4.5991E-14	**53**	$2p^{-2}2p^3 3p(1)3d$	33
113	$2p^5 3p\ (^3P)\ 3d\ ^4F_{9/2}$	3.7586E-12	**71**	$2p^{-2}2p^3 3p(2)3d$	48+20(105)
114	$2p^5 3p\ (^3P)\ 3d\ ^4D_{7/2}$	2.7629E-12	**81**	$2p^{-2}2p^3 3p(2)3d$	34+21(93)
115	$2p^5 3p\ (^1P)\ 3d\ ^2P_{3/2}$	3.9191E-14	**70**	$2p^{-2}2p^3 3p(1)3d$	29
116	$2p^5 3p\ (^1D)\ 3d\ ^2S_{1/2}$	1.8757E-14	**90**	$2p^{-2}2p^3 3p(2)3d$	29+41(96)
117	$2p^5 3p\ (^3D)\ 3d\ ^2G_{9/2}$	2.8431E-12	**62**	$2p^{-2}2p^3 3p(3)3d$	44+29(105)
118	$2p^5 3p\ (^1P)\ 3d\ ^2F_{7/2}$	3.0637E-12	**49**	$2p^{-2}2p^3 3p(3)3d$	18+27(102)+18(108)
119	$2p^5 3p\ (^3D)\ 3d\ ^2D_{5/2}$	3.3088E-15	**41**	$2p^{-2}2p^3 3p(3)3d$	31
120	$2p^5 3s\ (^3P)\ 3p\ ^4S_{3/2}$	1.0925E-14	**48**	$2p^{-1}2p^4 3s(0)3p$	21+35(41)
121	$2p^5 3p\ (^1S)\ 3d\ ^2D_{3/2}$	2.2955E-14	**87**	$2p^{-2}2p^3 3p(0)3d^{-1}$	49
122	$2p^5 3s\ (^1P)\ 3p\ ^2D_{5/2}$	9.4677E-13	**65**	$2p^{-1}2p^4 3s(1)3p$	20+26(42)
123	$2p^5 3p\ (^1D)\ 3d\ ^2P_{3/2}$	1.5378E-14	**79**	$2p^{-2}2p^3 3p(2)3d$	21+19(90)
124	$2p^5 3p\ (^3D)\ 3d\ ^2P_{3/2}$	1.7112E-15	**54**	$2p^{-2}2p^3 3p(3)3d$	36
125	$2p^5 3p\ (^3P)\ 3d\ ^2D_{5/2}$	2.4016E-15	**59**	$2p^{-2}2p^3 3p(2)3d$	25
126	$2p^5 3p\ (^3D)\ 3d\ ^2S_{1/2}$	1.6169E-15	**76**	$2p^{-2}2p^3 3p(3)3d$	37
127	$2p^5 3p\ (^1S)\ 3d\ ^2D_{5/2}$	2.2108E-14	**97**	$2p^{-2}2p^3 3p(0)3d$	55
128	$2p^5 3s\ (^3P)\ 3p\ ^2P_{1/2}$	8.3950E-15	**78**	$2p^{-1}2p^4 3s(1)3p$	34
129	$2p^5 3p^2\ ^4D^o_{1/2}$	6.5093E-13	**98**	$2p^{-1}\ 2p^4 3p^{-2}$	36+21(67)
130	$2p^5 3s\ (^3P)\ 3p\ ^2D_{3/2}$	3.8814E-14	**62**	$2p^{-1}2p^4 3s(1)3p$	55
131	$2p^5 3d^2\ ^4D^o_{1/2}$	2.1830E-13	**87**	$2p^{-2}\ 2p^3 3d^{-2}$	88
132	$2p^5 3d^2\ ^4D^o_{3/2}$	2.4946E-13	**87**	$2p^{-2}\ 2p^3 3d^{-2}$	47
133	$2p^5 3d^2\ ^4F^o_{5/2}$	1.7391E-13	**92**	$2p^{-2}\ 2p^3 3d^{-2}$	39
134	$2p^5 3d^2\ ^2G^o_{7/2}$	1.7218E-12	**97**	$2p^{-2}\ 2p^3 3d^{-2}$	37+17(157)
135	$2p^5 3d^2\ ^4D^o_{5/2}$	1.1012E-12	**85**	$2p^{-2}2p^3 3d^{-1}3d$	35+17(140)
136	$2p^5 3d^2\ ^4P^o_{3/2}$	1.1535E-13	**80**	$2p^{-2}\ 2p^3 3d^{-2}$	30
137	$2p^5 3d^2\ ^4G^o_{9/2}$	3.8328E-12	**57**	$2p^{-2}2p^3 3d^{-1}3d$	70
138	$2p^5 3d^2\ ^4F^o_{7/2}$	1.3225E-13	**70**	$2p^{-2}2p^3 3d^{-1}3d$	47+16(147)
140	$2p^5 3d^2\ ^4P^o_{5/2}$	7.4955E-14	**56**	$2p^{-2}2p^3 3d^{-1}3d$	45
141	$2p^5 3p^2\ ^4P^o_{1/2}$	2.6506E-12	**98**	$2p^{-1}2p^4 3p^{-1}3p$	46+28(129)+24(53)
142	$2p^5 3d^2\ ^4G^o_{11/2}$	4.9085E-12	**89**	$2p^{-2}2p^3 3d^{-1}3d$	52+48(151)
143	$2p^5 3d^2\ ^2F^o_{7/2}$	3.5718E-12	**83**	$2p^{-2}2p^3 3d^{-1}3d$	18+27(134)
144	$2p^5 3p^2\ ^4D^o_{3/2}$	1.6820E-13	**94**	$2p^{-1}2p^4 3p^{-1}3p$	45
145	$2p^5 3p^2\ ^2F^o_{5/2}$	3.3128E-13	**83**	$2p^{-1}2p^4 3p^{-1}3p$	43
146	$2p^5 3d^2\ ^2S^o_{1/2}$	8.6181E-13	**79**	$2p^{-2}2p^3 3d^{-1}3d$	29+24(158)
147	$2p^5 3d^2\ ^4D^o_{7/2}$	3.0795E-13	**73**	$2p^{-2}2p^3 3d^{-1}3d$	22+20(157)
148	$2p^5 3d^2\ ^4D^o_{5/2}$	7.5318E-14	**52**	$2p^{-2}2p^3 3d^{-1}3d$	38
149	$2p^5 3d^2\ ^4F^o_{9/2}$	4.7752E-12	**43**	$2p^{-2}2p^3 3d^{-1}3d$	40+25(155)
150	$2p^5 3d^2\ ^4S^o_{3/2}$	1.9793E-12	**63**	$2p^{-2}2p^3 3d^{-1}3d$	29+31(152)+17(136)
151	$2p^5 3d^2\ ^2H^o_{11/2}$	8.3232E-12	**89**	$2p^{-2}\ 2p^3 3d^2$	52+48(142)
152	$2p^5 3d^2\ ^2D^o_{3/2}$	2.3905E-15	**45**	$2p^{-2}2p^3 3d^{-1}3d$	20+21(159)
153	$2p^5 3d^2\ ^2D^o_{5/2}$	1.2682E-14	**59**	$2p^{-2}\ 2p^3 3d^2$	22
154	$2p^5 3d^2\ ^2F^o_{5/2}$	1.9253E-15	**27**	$2p^{-2}2p^3 3d^{-1}3d$	61
155	$2p^5 3d^2\ ^2G^o_{9/2}$	7.4131E-12	**79**	$2p^{-2}\ 2p^3 3d^2$	46+24(149)
156	$2p^5 3p^2\ ^2P^o_{3/2}$	5.7896E-15	**58**	$2p^{-1}2p^4 3p^{-1}3p$	19
157	$2p^5 3d^2\ ^2F^o_{7/2}$	9.7858E-15	**90**	$2p^{-2}\ 2p^3 3d^2$	46+39(147)
158	$2p^5 3d^2\ ^2P^o_{1/2}$	2.4576E-15	**68**	$2p^{-2}\ 2p^3 3d^2$	64
159	$2p^5 3s\ (^3P)\ 3d\ ^4F^o_{3/2}$	6.3751E-15	**28**	$2p^{-1}2p^4 3s(0)3d^{-1}$	42
160	$2p^5 3d^2\ ^2P^o_{1/2}$	2.1418E-15	**40**	$2p^{-2}2p^3 3d^{-1}3d$	56+20(146)
161	$2p^5 3s\ (^1P)\ 3d\ ^2F^o_{5/2}$	5.2170E-15	**62**	$2p^{-1}2p^4 3s(1)3d^{-1}$	17+36(62)
162	$2p^5 3d^2\ ^2G^o_{7/2}$	2.9746E-15	**75**	$2p^{-2}\ 2p^3 3d^2$	25+24(143)

The letter 'a' denotes unidentified level at position 97.

Table 2. Energies (in Ryd.) of lowest 162 fine structure levels of Ba XLVI

Level No.	Configurations	Energies (in Ryd.)				
		MCDF				FAC
		DC	Breit	QED	Total	
1	$2p^6 3s\ ^2S_{1/2}$	----	----	----	0.0000	0.0000
2	$2p^6 3p\ ^2P^o_{1/2}$	7.7945	0.1160	-0.1150	7.7954	7.7663
3	$2p^6 3p\ ^2P^o_{3/2}$	15.3721	0.0015	-0.1040	15.2700	15.2500
4	$2p^6 3d\ ^2D_{3/2}$	25.1758	-0.0432	-0.1140	25.0182	24.9801
5	$2p^6 3d\ ^2D_{5/2}$	26.9228	-0.1100	-0.1140	26.6980	26.6642
6	$2p^6 4s\ ^2S_{1/2}$	122.1405	-0.1000	-0.0705	121.9699	121.9502
7	$2p^6 4p\ ^2P^o_{1/2}$	125.3645	-0.0518	-0.1150	125.1979	125.1629
8	$2p^6 4p\ ^2P^o_{3/2}$	128.4497	-0.0988	-0.1100	128.2407	128.2095
9	$2p^6 4d\ ^2D_{3/2}$	132.1714	-0.1190	-0.1140	131.9377	131.8923
10	$2p^6 4d\ ^2D_{5/2}$	132.9256	-0.1450	-0.1140	132.6666	132.6234
11	$2p^6 4f\ ^2F^o_{5/2}$	134.8810	-0.1630	-0.1140	134.6033	134.5854
12	$2p^6 4f\ ^2F^o_{7/2}$	135.1973	-0.1670	-0.1140	134.9156	134.8971
13	$2p^6 5s\ ^2S_{1/2}$	176.4192	-0.1250	-0.0934	176.2005	176.1512
14	$2p^6 5p\ ^2P^o_{1/2}$	178.0410	-0.1010	-0.1150	177.8251	177.7683
15	$2p^6 5p\ ^2P^o_{3/2}$	179.5901	-0.1240	-0.1120	179.3532	179.2976
16	$2p^6 5d\ ^2D_{3/2}$	181.4133	-0.1350	-0.1140	181.1643	181.1022
17	$2p^6 5d\ ^2D_{5/2}$	181.8015	-0.1470	-0.1140	181.5403	181.4790
18	$2p^6 5f\ ^2F^o_{5/2}$	182.7651	-0.1550	-0.1140	182.4954	182.4529
19	$2p^6 5f\ ^2F^o_{7/2}$	182.9283	-0.1580	-0.1140	182.6559	182.6129
20	$2p^6 5g\ ^2G_{7/2}$	183.0604	-0.1590	-0.1140	182.7873	182.7353
21	$2p^6 5g\ ^2G_{9/2}$	183.1563	-0.1590	-0.1140	182.8830	182.8310
22	$2p^6 6s\ ^2S_{1/2}$	205.2743	-0.1010	-0.1030	205.0706	204.8722
23	$2p^6 6p\ ^2P^o_{1/2}$	206.2004	-0.0878	-0.1140	205.9982	205.7999
24	$2p^6 6p\ ^2P^o_{3/2}$	207.0856	-0.1000	-0.1130	206.8720	206.6838
25	$2p^6 6d\ ^2D_{3/2}$	208.1148	-0.1060	-0.1140	207.8945	207.7126
26	$2p^6 6d\ ^2D_{5/2}$	208.3397	-0.1130	-0.1140	208.1128	207.9375
27	$2p^6 6f\ ^2F^o_{5/2}$	208.8859	-0.1170	-0.1140	208.6542	208.4914
28	$2p^6 6f\ ^2F^o_{7/2}$	208.9807	-0.1190	-0.1140	208.7473	208.5862
29	$2p^6 6g\ ^2G_{7/2}$	209.0652	-0.1200	-0.1140	208.8311	208.6733
30	$2p^6 6g\ ^2G_{9/2}$	209.1208	-0.1200	-0.1140	208.8865	208.7287
31	$2p^6 7s\ ^2S_{1/2}$	222.3337	-0.1080	-0.1070	222.1184	221.9349
33	$2p^6 7p\ ^2P^o_{3/2}$	223.4636	-0.1080	-0.1140	223.2421	223.0652
34	$2p^6 7d\ ^2D_{3/2}$	224.1018	-0.1110	-0.1140	223.8761	223.7030
35	$2p^6 7d\ ^2D_{5/2}$	224.2434	-0.1150	-0.1140	224.0137	223.8447
36	$2p^6 7f\ ^2F^o_{5/2}$	224.5832	-0.1180	-0.1140	224.3506	224.1863
37	$2p^6 7f\ ^2F^o_{7/2}$	224.6431	-0.1190	-0.1140	224.4094	224.2462
38	$2p^6 7g\ ^2G_{7/2}$	224.6994	-0.1200	-0.1140	224.4652	224.3086
39	$2p^6 7g\ ^2G_{9/2}$	224.7344	-0.1200	-0.1140	224.5001	224.3434
40	$2p^5 3s^2\ ^2P^o_{3/2}$	333.6535	-0.5880	0.0661	333.1315	333.2115
41	$2p^5 3s\ (^3P)\ 3p\ ^4P_{3/2}$	339.6548	-0.4500	-0.0460	339.1589	339.2151
42	$2p^5 3s\ (^3P)\ 3p\ ^4D_{5/2}$	340.4228	-0.5020	-0.0461	339.8746	339.9307
43	$2p^5 3s\ (^1P)\ 3p\ ^2D_{3/2}$	340.6085	-0.4750	-0.0459	340.0873	340.1534
44	$2p^5 3s\ (^1P)\ 3p\ ^2P_{1/2}$	340.7210	-0.4280	-0.0465	340.2461	340.3100
45	$2p^5 3s\ (^3P)\ 3p\ ^4D_{7/2}$	347.1403	-0.6230	-0.0347	346.4826	346.5377
46	$2p^5 3s\ (^1P)\ 3p\ ^2P_{3/2}$	347.5434	-0.5890	-0.0348	346.9195	346.9827
47	$2p^5 3s\ (^3P)\ 3p\ ^4P_{5/2}$	347.8039	-0.5730	-0.0349	347.1958	347.2632
48	$2p^5 3s\ (^1P)\ 3p\ ^2S_{1/2}$	348.3346	-0.5870	-0.0357	347.7117	347.7733
49	$2p^5 3p^2\ ^4P^o_{3/2}$	348.6408	-0.3450	-0.1590	348.1367	348.1798
50	$2p^5 3s\ (^3P)\ 3p\ ^2D_{5/2}$	349.4580	-0.6040	-0.0361	348.8174	348.8744
51	$2p^5 3s\ (^3P)\ 3p\ ^2P_{3/2}$	349.8085	-0.5640	-0.0361	349.2086	349.2706
52	$2p^5 3s\ (^3P)\ 3p\ ^2S_{1/2}$	351.5262	-0.5120	-0.0352	350.9790	351.0391
53	$2p^5 3p^2\ ^2S^o_{1/2}$	355.2837	-0.4670	-0.1400	354.6766	354.7164

54	$2p^5\,3p^2\,{}^4P^o_{5/2}$	355.3322	-0.4620	-0.1470	354.7228	354.7618
55	$2p^5\,3p^2\,{}^2P^o_{3/2}$	355.4240	-0.4940	-0.1370	354.7924	354.8345
56	$2p^5\,3p^2\,{}^2F^o_{7/2}$	355.4366	-0.5510	-0.1330	354.7525	354.7963
57	$2p^5\,3p^2\,{}^2D^o_{3/2}$	355.9471	-0.4350	-0.1480	355.3647	355.4142
58	$2p^5\,3p^2\,{}^2D^o_{5/2}$	355.9907	-0.4890	-0.1360	355.3659	355.4165
59	$2p^5 3s\,(^3P)\,3d\,{}^4P^o_{1/2}$	356.8359	-0.5240	-0.0493	356.2623	356.2831
60	$2p^5 3s\,(^3P)\,3d\,{}^4P^o_{3/2}$	357.4289	-0.5930	-0.0482	356.7873	356.8070
61	$2p^5 3s\,(^1P)\,3d\,{}^2P^o_{1/2}$	357.5955	-0.5290	-0.0789	356.9872	357.0203
62	$2p^5 3s\,(^3P)\,3d\,{}^4F^o_{5/2}$	357.7950	-0.6470	-0.0458	357.1021	357.1260
63	$2p^5 3s\,(^3P)\,3d\,{}^4F^o_{7/2}$	357.9957	-0.6790	-0.0523	357.2648	357.2863
64	$2p^5 3s\,(^3P)\,3d\,{}^4D^o_{5/2}$	358.3846	-0.6230	-0.0518	357.7101	357.7360
65	$2p^5 3s\,(^1P)\,3d\,{}^2D^o_{3/2}$	358.4105	-0.5900	-0.0487	357.7720	357.7994
66	$2p^5 3s\,(^3P)\,3d\,{}^4F^o_{9/2}$	359.0635	-0.7400	-0.0453	358.2780	358.3010
67	$2p^5 3p^2\,{}^2P^o_{1/2}$	359.5413	-0.4650	-0.1120	358.9639	358.9900
69	$2p^5 3s\,(^3P)\,3d\,{}^4D^o_{7/2}$	359.9722	-0.6850	-0.0453	359.2417	359.2661
70	$2p^5 3s\,(^3P)\,3d\,{}^2F^o_{7/2}$	360.2440	-0.6920	-0.0632	359.4885	359.5174
71	$2p^5 3s\,(^3P)\,3d\,{}^2D^o_{3/2}$	360.2889	-0.6460	-0.0547	359.5878	359.6151
72	$2p^5 3s\,(^1P)\,3d\,{}^2D^o_{5/2}$	360.7416	-0.6480	-0.0634	360.0300	360.0587
73	$2p^5 3s\,(^3P)\,3d\,{}^2P^o_{1/2}$	361.7403	-0.7460	-0.0342	360.9597	361.0240
74	$2p^5 3s\,(^3P)\,3d\,{}^2P^o_{3/2}$	361.9445	-0.7030	-0.0494	361.1919	361.2120
75	$2p^5 3s^2\,{}^2P^o_{1/2}$	362.9612	-0.8830	0.0557	362.1338	362.2077
76	$2p^5 3p\,(^3P)\,3d\,{}^4D_{1/2}$	363.6237	-0.3910	-0.1600	363.0719	363.0752
77	$2p^5 3p^2\,{}^4D^o_{7/2}$	363.9332	-0.6260	-0.1300	363.1776	363.2166
78	$2p^5 3p^2\,{}^2P^o_{1/2}$	363.9886	-0.6250	-0.1050	363.2589	363.2904
79	$2p^5 3p^2\,{}^2D^o_{5/2}$	364.0576	-0.6060	-0.1270	363.3250	363.3618
80	$2p^5 3p\,(^3S)\,3d\,{}^4D_{3/2}$	364.1619	-0.4580	-0.1600	363.5434	363.5471
81	$2p^5 3p\,(^3D)\,3d\,{}^4G_{7/2}$	364.4859	-0.5770	-0.1600	363.7486	363.7564
82	$2p^5 3p\,(^3P)\,3d\,{}^4F_{5/2}$	364.5871	-0.4840	-0.1600	363.9425	363.9453
83	$2p^5 3p^2\,{}^2P^o_{3/2}$	365.0635	-0.5630	-0.1360	364.3636	364.4103
84	$2p^5 3p\,(^3D)\,3d\,{}^4P_{1/2}$	365.6235	-0.4550	-0.1600	365.0079	365.0112
85	$2p^5 3p\,(^3D)\,3d\,{}^4F_{5/2}$	366.1487	-0.5230	-0.1600	365.4656	365.4665
86	$2p^5 3p\,(^3D)\,3d\,{}^4D_{3/2}$	366.2553	-0.4740	-0.1600	365.6220	365.6223
87	$2p^5 3p^2\,{}^2D^o_{3/2}$	366.3724	-0.5300	-0.1350	365.7074	365.7571
88	$2p^5 3p\,(^3P)\,3d\,{}^4F_{7/2}$	366.7178	-0.5720	-0.1600	365.9852	365.9912
89	$2p^5 3p\,(^3D)\,3d\,{}^4G_{9/2}$	366.9580	-0.6440	-0.1600	366.1543	366.1658
90	$2p^5 3p\,(^3P)\,3d\,{}^2P_{3/2}$	367.0852	-0.5340	-0.1600	366.3907	366.3961
91	$2p^5 3p\,(^3P)\,3d\,{}^2F_{5/2}$	367.1194	-0.5540	-0.1600	366.4051	366.4125
92	$2p^5 3p\,(^3P)\,3d\,{}^4P_{5/2}$	367.5548	-0.5420	-0.1600	366.8524	366.8563
93	$2p^5 3p\,(^1D)\,3d\,{}^2F_{7/2}$	367.7038	-0.5810	-0.1600	366.9632	366.9707
94	$2p^5 3s\,(^3P)\,3p\,{}^4D_{1/2}$	368.7128	-0.8530	-0.0326	367.8268	367.8992
95	$2p^5 3s\,(^3P)\,3p\,{}^4D_{3/2}$	368.9207	-0.7260	-0.1130	368.0821	368.1323
96	$2p^5 3p\,(^3P)\,3d\,{}^2P_{1/2}$	369.4287	-0.6460	-0.1260	368.6570	368.6630
97	a	369.8515	-0.7810	-0.0485	369.0219	369.0507
98	$2p^5 3s\,(^3P)\,3p\,{}^4P_{1/2}$	371.6547	-0.8160	-0.0071	370.8317	370.9112
99	$2p^5 3p\,(^3D)\,3d\,{}^4P_{3/2}$	372.2128	-0.5340	-0.1490	371.5298	371.5350
100	$2p^5 3p\,(^1P)\,3d\,{}^2P_{1/2}$	372.3907	-0.5880	-0.1490	371.6538	371.6604
101	$2p^5 3p\,(^3D)\,3d\,{}^4D_{5/2}$	372.5678	-0.6110	-0.1490	371.8078	371.8136
102	$2p^5 3p\,(^3D)\,3d\,{}^2F_{7/2}$	372.7076	-0.6630	-0.1490	371.8954	371.9005
103	$2p^5 3p\,(^1P)\,3d\,{}^2F_{5/2}$	372.9276	-0.6610	-0.1490	372.1176	372.1215
105	$2p^5 3p\,(^3D)\,3d\,{}^4F_{9/2}$	373.1031	-0.7140	-0.1490	372.2396	372.2440
106	$2p^5 3p\,(^3D)\,3d\,{}^4G_{11/2}$	373.4266	-0.7650	-0.1490	372.5128	372.5246
107	$2p^5 3p\,(^3P)\,3d\,{}^4D_{3/2}$	373.5014	-0.5930	-0.1490	372.7601	372.7693
108	$2p^5 3p\,(^3D)\,3d\,{}^4D_{7/2}$	373.6255	-0.6440	-0.1490	372.8322	372.8426
109	$2p^5 3p\,(^3P)\,3d\,{}^4D_{5/2}$	373.7331	-0.6000	-0.1490	372.9846	372.9930
110	$2p^5 3p\,(^3P)\,3d\,{}^4P_{1/2}$	373.7692	-0.5710	-0.1490	373.0497	373.0573

111	$2p^5 3p\ (^3S)\ 3d\ ^4D_{7/2}$	373.8359	-0.6980	-0.1490	372.9889	372.9979
112	$2p^5 3p\ (^1P)\ 3d\ ^2D_{5/2}$	374.3386	-0.6940	-0.1490	373.4958	373.5025
113	$2p^5 3p\ (^3P)\ 3d\ ^4F_{9/2}$	374.5038	-0.6820	-0.1490	373.6729	373.6879
114	$2p^5 3p\ (^3P)\ 3d\ ^4D_{7/2}$	374.7599	-0.6810	-0.1490	373.9303	373.9441
115	$2p^5 3p\ (^1P)\ 3d\ ^2P_{3/2}$	374.9645	-0.6710	-0.1490	374.1444	374.1476
116	$2p^5 3p\ (^1D)\ 3d\ ^2S_{1/2}$	375.5240	-0.6390	-0.1480	374.7365	374.7495
117	$2p^5 3p\ (^3D)\ 3d\ ^2G_{9/2}$	375.5575	-0.7330	-0.1490	374.6752	374.6796
118	$2p^5 3p\ (^1P)\ 3d\ ^2F_{7/2}$	375.9857	-0.6830	-0.1490	375.1539	375.1545
119	$2p^5 3p\ (^3D)\ 3d\ ^2D_{5/2}$	376.1578	-0.8010	-0.1250	375.2316	375.2804
120	$2p^5 3s\ (^3P)\ 3p\ ^4S_{3/2}$	376.3191	-0.9200	-0.0335	375.3658	375.4572
121	$2p^5 3p\ (^1S)\ 3d\ ^2D_{3/2}$	376.4546	-0.5590	-0.1270	375.7685	375.7672
122	$2p^5 3s\ (^1P)\ 3p\ ^2D_{5/2}$	376.6429	-0.8800	-0.0454	375.7170	375.7507
123	$2p^5 3p\ (^1D)\ 3d\ ^2P_{3/2}$	376.6978	-0.6520	-0.1380	375.9078	375.9139
124	$2p^5 3p\ (^3D)\ 3d\ ^2P_{3/2}$	377.3090	-0.7470	-0.1280	376.4341	376.4461
125	$2p^5 3p\ (^3P)\ 3d\ ^2D_{5/2}$	377.4454	-0.7250	-0.1180	376.6022	376.6109
126	$2p^5 3p\ (^3D)\ 3d\ ^2S_{1/2}$	377.5248	-0.7670	-0.1230	376.6342	376.6636
127	$2p^5 3p\ (^1S)\ 3d\ ^2D_{5/2}$	378.1972	-0.6110	-0.1480	377.4380	377.4457
128	$2p^5 3s\ (^3P)\ 3p\ ^2P_{1/2}$	378.6659	-0.8990	-0.0233	377.7435	377.7908
129	$2p^5 3p^2\ ^4D^o_{1/2}$	378.7135	-0.7650	-0.1160	377.8326	377.8895
130	$2p^5 3s\ (^3P)\ 3p\ ^2D_{3/2}$	378.7500	-0.9790	-0.0018	377.7688	377.8350
131	$2p^5 3d^2\ ^4D^o_{1/2}$	381.9779	-0.5940	-0.1600	381.2242	381.1958
132	$2p^5 3d^2\ ^4D^o_{3/2}$	382.0068	-0.5690	-0.1600	381.2783	381.2494
133	$2p^5 3d^2\ ^4F^o_{5/2}$	382.3843	-0.6520	-0.1600	381.5728	381.5444
134	$2p^5 3d^2\ ^2G^o_{7/2}$	382.5613	-0.7110	-0.1590	381.6904	381.6622
135	$2p^5 3d^2\ ^4D^o_{5/2}$	383.5979	-0.6320	-0.1600	382.8064	382.7812
136	$2p^5 3d^2\ ^4P^o_{3/2}$	383.7339	-0.6240	-0.1590	382.9502	382.9211
137	$2p^5 3d^2\ ^4G^o_{9/2}$	383.8873	-0.7730	-0.1600	382.9543	382.9296
138	$2p^5 3d^2\ ^4F^o_{7/2}$	383.9792	-0.7220	-0.1600	383.0980	383.0731
139	$2p^5 3d^2\ ^2D^o_{3/2}$	384.2397	-0.6740	-0.1590	383.4067	383.3808
141	$2p^5 3p^2\ ^4P^o_{1/2}$	384.4085	-0.8570	-0.1110	383.4410	383.4968
142	$2p^5 3d^2\ ^4G^o_{11/2}$	384.4300	-0.8390	-0.1600	383.4316	383.4094
143	$2p^5 3d^2\ ^2F^o_{7/2}$	384.5019	-0.7550	-0.1600	383.5869	383.5621
144	$2p^5 3p^2\ ^4D^o_{3/2}$	384.5398	-0.8920	-0.1030	383.5450	383.6028
145	$2p^5 3p^2\ ^2F^o_{5/2}$	384.6093	-0.9480	-0.0892	383.5716	383.6270
146	$2p^5 3d^2\ ^2S^o_{1/2}$	384.9627	-0.6670	-0.1600	384.1366	384.1091
147	$2p^5 3d^2\ ^4D^o_{7/2}$	385.1150	-0.7110	-0.1590	384.2442	384.2167
148	$2p^5 3d^2\ ^4D^o_{5/2}$	385.1870	-0.7030	-0.1590	384.3245	384.2973
149	$2p^5 3d^2\ ^4F^o_{9/2}$	385.2177	-0.7580	-0.1600	384.3004	384.2742
150	$2p^5 3d^2\ ^4S^o_{3/2}$	385.3675	-0.6610	-0.1590	384.5465	384.5179
151	$2p^5 3d^2\ ^2H^o_{11/2}$	385.8879	-0.8540	-0.1600	384.8747	384.8538
152	$2p^5 3d^2\ ^2D^o_{3/2}$	386.2114	-0.8630	-0.1170	385.2319	385.2534
153	$2p^5 3d^2\ ^2D^o_{5/2}$	386.2368	-0.7730	-0.1580	385.3058	385.2842
154	$2p^5 3d^2\ ^2F^o_{5/2}$	386.4810	-0.8130	-0.1360	385.5320	385.5368
155	$2p^5 3d^2\ ^2G^o_{9/2}$	386.4925	-0.7830	-0.1600	385.5504	385.5258
156	$2p^5 3p^2\ ^2P^o_{3/2}$	386.6024	-0.8830	-0.0775	385.6419	385.6812
157	$2p^5 3d^2\ ^2F^o_{7/2}$	386.6080	-0.8080	-0.1590	385.6409	385.6187
158	$2p^5 3d^2\ ^2P^o_{1/2}$	386.8066	-0.7640	-0.1540	385.8886	385.8739
159	$2p^5 3s\ (^3P)\ 3d\ ^4F^o_{3/2}$	386.9524	-0.9130	-0.0552	385.9841	386.0009
160	$2p^5 3d^2\ ^2P^o_{1/2}$	387.1434	-0.8070	-0.1420	386.1946	386.1814
161	$2p^5 3s\ (^1P)\ 3d\ ^2F^o_{5/2}$	387.3951	-0.9660	-0.0383	386.3903	386.4053
162	$2p^5 3d^2\ ^2G^o_{7/2}$	387.7032	-0.8090	-0.1510	386.7433	386.7267

Table 3. Comparison of our calculated lowest 21 fine structure levels of Ba XLVI with other references

Level No.	Configurations	Parity	Energies in Ryd.				
			MCDF	FAC	Ref.[33]	Ref.[18]	Ref.[13]
1	$2p^6 3s\ ^2S_{1/2}$	+	0.0000	0.0000	0.0000	0.0000	0.0000
2	$2p^6 3p\ ^2P^o_{1/2}$	-	7.7954	7.7663	7.7457	7.7161	7.7366
3	$2p^6 3p\ ^2P^o_{3/2}$	-	15.2700	15.2500	15.2319	15.1974	15.2973
4	$2p^6 3d\ ^2D_{3/2}$	+	25.0182	24.9801	24.9806	24.9453	25.0562
5	$2p^6 3d\ ^2D_{5/2}$	+	26.6980	26.6642	26.6710	26.6334	26.7964
6	$2p^6 4s\ ^2S_{1/2}$	+	121.9699	121.9502	121.9780	121.9119	122.2303
7	$2p^6 4p\ ^2P^o_{1/2}$	-	125.1979	125.1629	125.2080	125.0990	125.3700
8	$2p^6 4p\ ^2P^o_{3/2}$	-	128.2407	128.2095	128.2500	128.1461	128.4415
9	$2p^6 4d\ ^2D_{3/2}$	+	131.9377	131.8923	131.9450	131.8358	132.1588
10	$2p^6 4d\ ^2D_{5/2}$	+	132.6666	132.6234	132.6770	132.5690	132.9470
11	$2p^6 4f\ ^2F^o_{5/2}$	-	134.6033	134.5854	134.6120	134.5212	134.9196
12	$2p^6 4f\ ^2F^o_{7/2}$	-	134.9156	134.8971	134.9290	134.8353	135.2385
13	$2p^6 5s\ ^2S_{1/2}$	+	176.2005	176.1512	176.2070		176.4913
14	$2p^6 5p\ ^2P^o_{1/2}$	-	177.8251	177.7683	177.8270		178.3259
15	$2p^6 5p\ ^2P^o_{3/2}$	-	179.3532	179.2976	179.3580		179.9269
16	$2p^6 5d\ ^2D_{3/2}$	+	181.1643	181.1022	181.1640		181.6696
17	$2p^6 5d\ ^2D_{5/2}$	+	181.5403	181.4790	181.5420		182.0856
18	$2p^6 5f\ ^2F^o_{5/2}$	-	182.4954	182.4529	182.4950		182.6857
19	$2p^6 5f\ ^2F^o_{7/2}$	-	182.6559	182.6129	182.6560		182.8531
20	$2p^6 5g\ ^2G_{7/2}$	+	182.7873	182.7353	182.7970		
21	$2p^6 5g\ ^2G_{9/2}$	+	182.8830	182.8310	182.8930		

Table 4. Radiative data for E1 transitions in Ba XLVI ($aE \pm b = a \times 10^{\pm b}$)

Transition No.	i	j	λ (in Å)	A_{ji} (in s^{-1})	f_{ij}	s_{ij} (in a.u.)	vel/len
1	1	2	116.9000	2.55E+10	5.22E-02	4.02E-02	0.96
2	1	3	59.6770	2.00E+11	2.14E-01	8.41E-02	0.99
3	1	7	7.2786	1.55E+13	1.23E-01	5.91E-03	1.00
4	1	8	7.1059	1.22E+13	1.84E-01	8.63E-03	1.00
5	1	14	5.1245	8.72E+12	3.43E-02	1.16E-03	0.99
6	1	15	5.0809	7.27E+12	5.63E-02	1.88E-03	0.98
7	1	23	4.4237	5.15E+12	1.51E-02	4.40E-04	0.94
8	1	24	4.4050	4.41E+12	2.57E-02	7.45E-04	0.93
9	1	32	4.0920	3.48E+12	8.73E-03	2.35E-04	0.88
10	1	33	4.0820	3.07E+12	1.53E-02	4.12E-04	0.85
11	1	40	2.7355	2.99E+13	6.71E-02	1.21E-03	0.99
12	1	49	2.6176	4.29E+11	8.81E-04	1.52E-05	1.00
13	1	53	2.5693	2.61E+12	2.58E-03	4.36E-05	0.99
14	1	55	2.5685	4.68E+12	9.25E-03	1.56E-04	0.99
15	1	57	2.5643	7.65E+11	1.51E-03	2.55E-05	0.98
16	1	59	2.5579	1.41E+11	1.38E-04	2.32E-06	0.94
17	1	60	2.5541	4.95E+11	9.68E-04	1.63E-05	0.97
18	1	61	2.5527	2.99E+12	2.92E-03	4.91E-05	1.00
19	1	65	2.5471	2.76E+12	5.36E-03	9.00E-05	0.98
20	1	67	2.5386	1.31E+14	1.26E-01	2.11E-03	0.97
21	1	71	2.5342	1.70E+13	3.28E-02	5.48E-04	0.98
22	1	73	2.5246	5.01E+14	4.79E-01	7.95E-03	0.98
23	1	74	2.5230	7.55E+14	1.44E+00	2.39E-02	0.97
24	1	75	2.5164	5.91E+13	5.61E-02	9.30E-04	0.97
25	1	78	2.5086	1.18E+14	1.11E-01	1.84E-03	0.97
26	1	83	2.5010	2.74E+12	5.14E-03	8.47E-05	0.92
27	1	87	2.4918	1.03E+13	1.91E-02	3.13E-04	1.00
28	1	129	2.4118	8.00E+11	6.97E-04	1.11E-05	1.10
29	1	131	2.3904	6.60E+11	5.66E-04	8.90E-06	0.97
30	1	132	2.3900	6.02E+11	1.03E-03	1.62E-05	0.97
31	1	136	2.3796	2.40E+11	4.07E-04	6.37E-06	0.97
32	1	139	2.3768	4.96E+10	8.40E-05	1.32E-06	1.00
33	1	141	2.3766	1.18E+11	1.00E-04	1.57E-06	0.99
34	1	144	2.3759	4.93E+12	8.35E-03	1.31E-04	0.98
35	1	146	2.3723	2.50E+11	2.11E-04	3.30E-06	0.96
36	1	150	2.3697	3.39E+10	5.71E-05	8.91E-07	0.94
37	1	152	2.3655	6.67E+12	1.12E-02	1.74E-04	0.98
38	1	156	2.3630	4.19E+13	7.02E-02	1.09E-03	0.96
39	1	158	2.3615	4.16E+13	3.48E-02	5.41E-04	0.98
40	1	159	2.3609	7.25E+10	1.21E-04	1.88E-06	0.76
41	1	160	2.3596	8.76E+13	7.31E-02	1.14E-03	0.98

Table 5. Radiative data for E2 transition in Ba XLVI ($aE \pm b = a \times 10^{\pm b}$)

Transition	i	j	λ (in Å)	A_{ji} (in s^{-1})	f_{ij}	s_{ij} (in a.u.)	vel/len
1	1	4	36.4240	1.27E+07	5.04E-06	2.90E-03	1.00
2	1	5	34.1330	1.80E+07	9.42E-06	4.46E-03	1.00
3	1	9	6.9068	5.87E+10	8.39E-04	3.29E-03	1.00
4	1	10	6.8689	5.86E+10	1.24E-03	4.80E-03	1.00
5	1	16	5.0301	2.61E+10	1.98E-04	3.00E-04	0.97
6	1	17	5.0197	2.68E+10	3.04E-04	4.58E-04	0.97
7	1	25	4.3833	1.43E+10	8.25E-05	8.28E-05	0.86
8	1	26	4.3787	1.49E+10	1.29E-04	1.29E-04	0.86
9	1	34	4.0704	1.46E+10	7.25E-05	5.82E-05	0.46
10	1	35	4.0679	1.53E+10	1.14E-04	9.13E-05	0.46
11	1	41	2.6869	3.73E+10	8.07E-05	1.86E-05	0.99
12	1	42	2.6812	1.27E+11	4.09E-04	9.40E-05	0.99
13	1	43	2.6795	1.30E+11	2.80E-04	6.42E-05	0.98
14	1	46	2.6267	2.13E+10	4.40E-05	9.49E-06	0.98
15	1	47	2.6247	1.24E+11	3.84E-04	8.26E-05	0.98
16	1	50	2.6125	3.44E+10	1.06E-04	2.24E-05	0.99
17	1	51	2.6095	1.00E+11	2.04E-04	4.33E-05	0.99
18	1	80	2.5066	4.68E+07	8.82E-08	1.65E-08	1.00
19	1	82	2.5039	4.88E+08	1.38E-06	2.57E-07	0.99
20	1	85	2.4935	1.45E+09	4.06E-06	7.50E-07	1.00
21	1	86	2.4924	1.36E+08	2.54E-07	4.68E-08	1.00
22	1	90	2.4872	1.11E+08	2.06E-07	3.77E-08	1.10
23	1	91	2.4871	3.71E+07	1.03E-07	1.89E-08	1.10
24	1	92	2.4840	8.87E+08	2.46E-06	4.49E-07	1.00
25	1	95	2.4757	9.98E+08	1.84E-06	3.32E-07	0.85
26	1	97	2.4694	2.97E+09	5.42E-06	9.73E-07	1.00
27	1	99	2.4528	1.98E+08	3.57E-07	6.27E-08	1.10
28	1	101	2.4509	1.48E+06	4.00E-09	7.01E-10	0.84
29	1	103	2.4489	1.35E+09	3.64E-06	6.37E-07	1.00
30	1	104	2.4481	3.16E+08	5.68E-07	9.92E-08	1.10
31	1	107	2.4447	3.79E+08	6.79E-07	1.18E-07	0.99
32	1	109	2.4432	2.37E+07	6.35E-08	1.10E-08	1.00
33	1	112	2.4398	1.46E+07	3.91E-08	6.77E-09	0.77
34	1	115	2.4356	9.53E+08	1.69E-06	2.92E-07	1.00
35	1	119	2.4286	5.50E+10	1.46E-04	2.49E-05	0.97
36	1	120	2.4277	8.61E+09	1.52E-05	2.59E-06	0.98
37	1	121	2.4251	2.00E+08	3.53E-07	5.99E-08	1.10
38	1	122	2.4254	9.51E+10	2.52E-04	4.28E-05	0.99
39	1	123	2.4242	3.02E+08	5.33E-07	9.04E-08	1.00
40	1	124	2.4208	2.66E+10	4.68E-05	7.91E-06	1.00
41	1	125	2.4197	1.61E+10	4.24E-05	7.15E-06	1.00
42	1	127	2.4144	2.81E+07	7.36E-08	1.23E-08	0.85
43	1	130	2.4122	1.20E+11	2.09E-04	3.50E-05	0.98

Table 6. Radiative data for M1 transition in Ba XLVI ($aE \pm b = a \times 10^{\pm b}$)

i	j	λ (in Å)	A_{ji} (in s^{-1})	f_{ij}	s_{ij} (in a.u.)
1	3	59.6770	6.30E+03	6.73E-09	1.28E+00
1	8	7.1059	2.63E+07	3.99E-07	1.28E-01
1	11	6.7700	1.35E+02	2.79E-12	7.74E-07
1	15	5.0809	3.06E+07	2.37E-07	2.78E-02
1	18	4.9934	6.34E+01	7.11E-13	7.92E-08
1	24	4.4050	2.47E+07	1.44E-07	1.10E-02
1	27	4.3674	2.38E+01	2.04E-13	1.52E-08
1	33	4.0820	2.00E+07	1.00E-07	6.08E-03
1	36	4.0618	1.19E+02	8.85E-13	5.30E-08
1	40	2.7355	3.87E+08	8.69E-07	1.59E-02
1	49	2.6176	1.43E+06	2.94E-09	4.72E-05
1	54	2.5690	1.83E+06	5.42E-09	8.22E-05
1	55	2.5685	3.85E+08	7.61E-07	1.15E-02
1	57	2.5643	4.21E+07	8.30E-08	1.25E-03
1	58	2.5643	3.36E+07	9.93E-08	1.50E-03
1	60	2.5541	3.85E+08	7.53E-07	1.12E-02
1	62	2.5518	6.74E+07	1.98E-07	2.94E-03
1	64	2.5475	1.11E+09	3.24E-06	4.80E-02
1	65	2.5471	4.49E+08	8.74E-07	1.29E-02
1	68	2.5390	9.00E+09	2.61E-05	3.82E-01
1	71	2.5342	8.64E+09	1.66E-05	2.42E-01
1	72	2.5311	2.14E+07	6.16E-08	8.94E-04
1	74	2.5230	9.12E+07	1.74E-07	2.50E-03
1	79	2.5081	6.43E+07	1.82E-07	2.57E-03
1	83	2.5010	2.78E+07	5.22E-08	7.31E-04
1	87	2.4918	2.12E+08	3.95E-07	5.46E-03
1	132	2.3900	1.19E+06	2.04E-09	2.49E-05
1	133	2.3882	1.34E+05	3.44E-10	4.19E-06
1	135	2.3805	2.60E+06	6.63E-09	8.00E-05
1	136	2.3796	2.32E+04	3.93E-11	4.74E-07
1	139	2.3768	6.07E+06	1.03E-08	1.24E-04
1	140	2.3763	1.06E+07	2.69E-08	3.23E-04
1	144	2.3759	3.69E+07	6.24E-08	7.49E-04
1	145	2.3758	2.34E+07	5.93E-08	7.11E-04
1	148	2.3711	4.89E+05	1.24E-09	1.47E-05
1	150	2.3697	3.95E+06	6.65E-09	7.92E-05
1	152	2.3655	1.29E+08	2.16E-07	2.56E-03
1	153	2.3651	6.45E+05	1.62E-09	1.92E-05
1	154	2.3637	5.44E+07	1.37E-07	1.61E-03
1	156	2.3630	1.44E+07	2.41E-08	2.84E-04
1	159	2.3609	5.06E+08	8.46E-07	9.97E-03
1	161	2.3584	4.30E+07	1.08E-07	1.26E-03

Table 7. Radiative data for M2 transition in Ba XLVI ($aE \pm b = a \times 10^{\pm b}$)

i	j	λ (in Å)	A_{ji} (in s^{-1})	f_{ij}	s_{ij} (in a.u.)
1	4	36.4240	3.93E+02	1.56E-10	2.81E-06
1	6	7.4713	2.06E+06	1.72E-08	6.36E-05
1	9	6.9068	3.43E+04	4.91E-10	1.68E-06
1	13	5.1718	2.47E+06	9.91E-09	2.53E-05
1	16	5.0301	4.77E+04	3.62E-10	9.00E-07
1	22	4.4437	1.75E+06	5.18E-09	1.14E-05
1	25	4.3833	3.48E+04	2.00E-10	4.34E-07
1	31	4.1026	7.70E+05	1.94E-09	3.94E-06
1	34	4.0704	1.26E+04	6.26E-11	1.26E-07
1	41	2.6869	9.99E+08	2.16E-06	2.87E-03
1	43	2.6795	4.51E+08	9.72E-07	1.29E-03
1	44	2.6783	1.21E+09	1.30E-06	1.72E-03
1	46	2.6267	3.02E+08	6.24E-07	8.11E-04
1	48	2.6208	5.69E+08	5.86E-07	7.59E-04
1	51	2.6095	1.02E+07	2.08E-08	2.69E-05
1	52	2.5964	6.59E+07	6.66E-08	8.55E-05
1	76	2.5099	4.50E+04	4.25E-11	5.27E-08
1	80	2.5066	1.25E+05	2.35E-10	2.91E-07
1	84	2.4966	6.28E+06	5.87E-09	7.24E-06
1	86	2.4924	9.51E+05	1.77E-09	2.18E-06
1	90	2.4872	1.74E+05	3.23E-10	3.97E-07
1	94	2.4774	2.74E+07	2.53E-08	3.09E-05
1	95	2.4757	3.25E+07	5.96E-08	7.30E-05
1	96	2.4719	2.26E+05	2.07E-10	2.54E-07
1	97	2.4694	3.75E+07	6.85E-08	8.37E-05
1	98	2.4574	1.74E+07	1.57E-08	1.91E-05
1	99	2.4528	1.93E+06	3.47E-09	4.21E-06
1	100	2.4519	8.72E+02	7.86E-13	9.53E-10
1	104	2.4481	1.95E+06	3.51E-09	4.25E-06
1	107	2.4447	1.37E+05	2.46E-10	2.98E-07
1	110	2.4428	1.04E+06	9.31E-10	1.12E-06
1	115	2.4356	3.21E+06	5.72E-09	6.89E-06
1	116	2.4318	7.97E+06	7.06E-09	8.50E-06
1	120	2.4277	8.00E+08	1.41E-06	1.70E-03
1	121	2.4251	1.52E+07	2.68E-08	3.21E-05
1	123	2.4242	1.49E+07	2.62E-08	3.14E-05
1	124	2.4208	2.06E+07	3.62E-08	4.34E-05
1	126	2.4195	1.61E+08	1.42E-07	1.69E-04
1	128	2.4124	6.29E+08	5.49E-07	6.55E-04
1	130	2.4122	6.84E+07	1.19E-07	1.42E-04

4. Lifetimes

The lifetime τ of a level j can be determined from the reciprocal of the sum of transition probabilities of radiative transitions from level i as

$$\tau_j(s) = \frac{1}{\sum_i A_{ji}(s^{-1})}. \tag{4.1}$$

In Table 1, inverse radiative rates for the lowest 162 fine-structure levels for Ba XLVI calculated by including all possible E1 (electric dipole), M1 (magnetic dipole), E2 (electric quadrupole) and M2 (magnetic quadrupole) transitions have been listed. As no calculations or measurements for lifetimes in Na-like Barium are available in the literature, therefore inverse radiative rates reported in the present paper will be beneficial for future comparisons.

5. Conclusion

Motivated by the need of accurate and large amount of atomic data, in the present work, the energy levels and inverse radiative rates for the lowest 162 fine structure levels belonging to the configurations $2p^6 3l$ (l=0-2), $2p^6 4l$ (l=0-3), $2p^6 5l$ (l=0-4), $2p^6 6l$ (l=0-4), $2p^6 7l$ (l=0-4), $2p^5 3l^2$ (l=0,1), $2p^5 3s3p$, 2p53s3d and 2p53p3d for Ba XLVI have been computed from MCDF method. Moreover, we have presented the radiative data i.e. radiative rates, transition wavelengths, oscillator strengths and line strengths for E1 and M1 transitions from the ground state. Two calculations have been performed, using the GRASP and MCDF codes. A comparison has been made between the two sets of energy levels, as well as with the available NIST-compiled values, showing a satisfactory agreement in general. The vel/len ratio of oscillator strength reaffirms the accuracy of our calculations. Further, EUV and SXR spectral lines in dipole and quadrupole transitions have also been identified. Hopefully, work in the present paper is comprehensive and may be useful in the diagnosis and classification of EUV and SXR spectral lines. Moreover, the present wide range of data may be beneficial in fusion, astrophysical plasma and plasma modelling.

Acknowledgement

I express my deep sense of gratitude to Prof. Man Mohan, Department of Physics and Astrophysics, University of Delhi for his inspiring and valuable guidance, fruitful discussions, motivation and persistent as well as continuous encouragement throughout this research work. I am also thankful to Kirori Mal College, University of Delhi for providing necessary infrastructure and facilities for the work.

Competing Interests

The author declares that he has no competing interests.

Authors' Contributions

The author wrote, read and approved the final manuscript.

References

[1] Chandra X-ray Observatory, available at `http://chandra.harvard.edu/`

[2] The Solar and Heliospheric Observatory, available at `http://sohowww.nascom.nasa.gov/`

[3] M.F. Gu, *Astrophys. J.* **582** (2003), 1241.

[4] P. Desai, *Astrophys. J.* **625** (2005), L59.

[5] H. Chen, *Astrophys. J.* **646**, 653.

[6] M.F. Gu, R. Gupta, J.R. Peterson, M. Sako and S.M. Kahn, *Astrophys. J.* **649** 979 (2006).

[7] F.P. Keenan, J.J. Drake and K.M. Aggarwal, *Mon. Not. R. Astron. Soc.* **381** (2007), 1727.

[8] D.H. Sampson, H.L. Jhang and C.J. Fontes, *At. Data and Nucl. Data Tables* **44** (1990), 209 – 271.

[9] W.O. Younis, S.H. Allam and Th.M. El-Sherbini, *At. Data Nucl. Data Tables* **92** (2006), 187 – 205.

[10] J. Reader, J.D. Gillaspy, D. Osin and Y.J. Ralchenko, *J. Phys. B: At. Mol. Opt. Phys.* **47** 145003 (2014), 12.

[11] L.-U. Crespo Jr., P. Beiersdorfer, K. Widmann and V. Decaux, *Phys. Scr. T* **80** (1999), 448.

[12] L.-U. Crespo Jr., P. Beiersdorfer, K. Widmann and V. Decaux, *Can. J. Phys.* **80** (2002), 1687.

[13] L.N. Ivanov and E.P. Ivanova, *At. Data and Nucl. Data Tables* **24** (1979), 95 – 109.

[14] C.E. Theodosiou and L.J. Curtis, *Phys. Rev. A* **38** (1988), 4435.

[15] J.F. Seely and R.A. Wagner, *Phys. Rev. A* **41** (1990), 5246(R).

[16] Y.K. Kim, D.H. Baik, P. Indelicato and J.P. Desclaux, *Phys. Rev. A* **44** (1991), 148.

[17] J.F. Seely, C.M. Brown, U. Feldman and J.O. Ekberg, *At. Data and Nucl. Data Tables* **47** (1991), 1 – 15.

[18] D.H. Baik, Y.G. Ohr, K.S. Kim and J.M. Lee, *At. Data and Nucl. Data Tables* **47** (1991), 177 – 203.

[19] W.R. Johnson, Z.W. Liu and J. Sapirstein, *Atomic At. Data and Nucl. Data Tables* **64** (1996), 279 – 300.

[20] J. Sapirstein and K.T. Cheng, *Physical Review A* **68** (2003), 042111.

[21] J. Jiang, C.-Z. Dong and L.-Y. Xie, *Physical Review A* **78** (2008), 022709.

[22] J.E. Sansonetti and J.J. Curry, *J. Phys. Chem. Ref. Data* **39** (4) (2010).

[23] J.D. Gillaspy, D. Osin, Yu. Ralchenko, J. Reader and S.A. Blundell, *Physical Review A* **87** (2013), 062503.

[24] C.J. Fontes and H.L. Zhang, *At. Data and Nucl. Data Tables* **113** (2017), 293 – 315.

[25] P.H. Norrington, `http://www.am.qub.ac.uk/DARC/` (2009).

[26] I.P. Grant, B.J. McKenzie, P.H. Norrington, D.F. Mayers and N.C. Pyper, *Comput. Phys. Commun.* **21** (1980), 207.

[27] P. Jönsson, X. He, C.F. Fischer and I.P. Grant, *Comput. Phys. Commun.* **177** (2007), 597.

[28] F.A. Parpia, C.F. Fischer and I.P. Grant, *Comput. Phys. Commun.* **94** (1996), 249.

[29] J. Olsen, M.R. Godefroid, P. Jönsson, P.A. Malmqvist and C.F. Fischer, *Phys. Rev. E* **52** (1995), 4499.

[30] B. Frick, *Phys. Scr.* **T8** (1986), 129.

[31] M.F. Gu, *Can. J. Phys.* **86**, 675 (2008), 675.

[32] D.H. Sampson, H.L. Zhang and A.K. Mohanty, *Phys. Rev. A* **40** (2) (1989), 604 – 615.

[33] `http://physics.nist.gov/cgi-bin/ASD/energy1.pl`

[34] I.P. Grant, *J. Phys. B* **7** (1974), 1458.

[35] P. Marketos, *Z. Phys. D.* **29** (1994), 247.

[36] J.P. Santos, A.M. Costa, C. Madruga, F. Parente and P. Indelicato, *Eur. Phys. J. D* **63** (2011), 89.

[37] A. Ynnerman and C. Froese Fischer, *Phys. Rev. A* **51** (1995), 2020 – 2030.